Geophysical Research Letter

Supporting Information for

Scattering attenuation images of the control of thrusts and fluid overpressure on the 2016-17 Central Italy seismic sequence

Simona Gabrielli[1,2*], Aybige Akinci[1], Luca De Siena[2,3], Edoardo Del Pezzo[4,5], Mauro Buttinelli[1], Francesco Emanuele Maesano[1], and Roberta Maffucci[1]

[1] Istituto Nazionale di Geofisica e Vulcanologia, Rome, Italy.

[2] School of Geosciences, University of Aberdeen, Aberdeen, United Kingdom.

[3] Institute of Geosciences, Johannes Gutenberg University, University of Mainz, Mainz, Germany.

[4] Osservatorio Vesuviano, Istituto Nazionale di Geofisica e Vulcanologia, Napoli, Italy

[5] Istituto Andaluz de Geofisica, Universidad de Granada, Granada, Spain

Contents of this file

Introduction

In this Supplementary Information we provide a more detailed description of the dataset and of the technique applied in our research (Text S1) and the Supplementary figures regarding the dataset (rays – Figures S1,2), the technique (Figure S3) and an additional way of displaying the results for all the sequences used in this work at 1.5 Hz (Figures S4-8) and at 6Hz (Figures S9-S13).

Text S1.

Data Selection

We considered the dataset used by Akinci et al. (2020) and Gabrielli et al. (2022), both for the pre-sequence and the sequence time period. The dataset comprises weak- and strong-motion data from the Amatrice-Visso-Norcia (AVN) sequence, using earthquakes with magnitudes between 2.8 and 6.5. The weak- and strong-motion accelerograms are available from the Italian Accelerometric Archive (ITACA) website, the European Strong Motion (ESM) database, and the European Integrated Data Archive (EIDA) repository.
Both P- and S- waves have been manually picked, and all the stations with only one seismic event recorded have been excluded. We also removed all waveforms with a P-wave travel time higher than 35 s to constrain their propagation within the crust. Waveforms with spikes, telemetry gaps, and wave arrivals in the coda of the horizontal components of ground motion were manually removed. Moreover, the dataset comprises seismograms with a signal-to-noise ratio (SNR) higher than three.

We decreased the size of the area compared to the paper of Gabrielli et al. (2022), to focus on the main tectonic structures. To do so, we reduced the dataset, removing the stations outside the new grid. The actual grid goes between 12.7°-13.5° and 42.3°-43.3°. Earthquakes with a maximum depth of 20 km and a source-station distance shorter than 100 km have been evaluated.
Peak delay was applied on the horizontal E-W component, following Gabrielli et al. (2022), which demonstrated how the results for all components were almost identical. Therefore, we performed the analysis on the E component, allowing us to interpret and compare the 3D results with the 2D of Gabrielli et al. (2022).
The pre-sequence dataset (January 7, 2013 – August 23, 2016) comprises 4731 waveforms (362 events) recorded at 17 seismic stations (**Figure S1**), while the AVN dataset (August 24, 2016 – January 5, 2017) contains 5373 waveforms (655 events) recorded at 64 seismic stations (**Figure S2**).
To further evaluate the changes in scattering in time, we divided the seismic sequence into three time periods, each one related to a mainshock of 2016:

- the Amatrice sequence, recorded between August 24 and October 25, 2016 (~1470 waveforms);
- the Visso sequence, recorded between October 26 and October 29, 2016 (~320 waveforms);
- the Norcia sequence, between October 30 and January 5, 2017 (~3240 waveforms).

The seismograms are filtered with a band-pass Butterworth filter (fourth order) in 1-2 Hz frequency band with a central frequency corresponding to 1.5. Being Visso a smaller dataset, we restricted the grid between 12.85°-13.4° and 42.55°-43.3°, in order to focus only on the area illuminated by the events and by the ray coverage. Due to the small size of the dataset, we are not able to obtain an imaging at 12 km depth, as also shown by Figure 4 in section AA' in the main text.

Peak Delay Imaging

The peak delay time, defined as the time difference between the S-wave arrival and the maximum amplitude of the event (Takahashi et al., 2007) and it is considered as a measurement of multiple forward scattering due to random inhomogeneities in the crust (Takahashi et al., 2007; Calvet et al., 2013). We considered the horizontal E-W component of the seismograms considering the work of Gabrielli et al. (2022), where it was demonstrated how the different components of this dataset do not influence the results of peak delay calculations.
The dependence of peak delay time (tPD(r)) on the hypocentral distances (R) Is defined by

$$\log_{10}t^{PD}(f)=A(f)+B(f)\cdot\log_{10}R \qquad (1)$$

where *A(f)* and *B(f)* are the coefficient of the linear fit.

To obtain the ray length R, we use the 3D velocity model obtained by Pitarka et al. (2022) to propagate rays in the 3D grid, applying the ray-bending approach of MuRAT3.0 (De Siena et al. 2016, from Block, 1991). In **Figure S3** we plotted the measured peak delay times and their dependence on the hypocentral distances R (black circles), for the frequency band 1-2 Hz, and for the sequence dataset. Red line represents the linear regression defined by (1).
The difference between the measured peak delay time of the ith waveform and the theoretical measurement gives the amount of scattering accumulated along the ray path:

$$\log_{10}t(f) = \log_{10}t_i^{PD}(f) - \log_{10}t^{PD}(f) \qquad (2)$$

Negative values of log10t(f) represent low scattering zones, indicating rigid and compact crust; positive values mark high-scattering areas, indicating the crust's highly fractured and heterogenous areas.

To map peak delay, we used a regionalization approach. The area has been divided into a grid with blocks of 2.5 km × 2.5 km horizontally and 1 km vertically. For each cell, we calculated the average peak delay for all the rays crossing the cell.

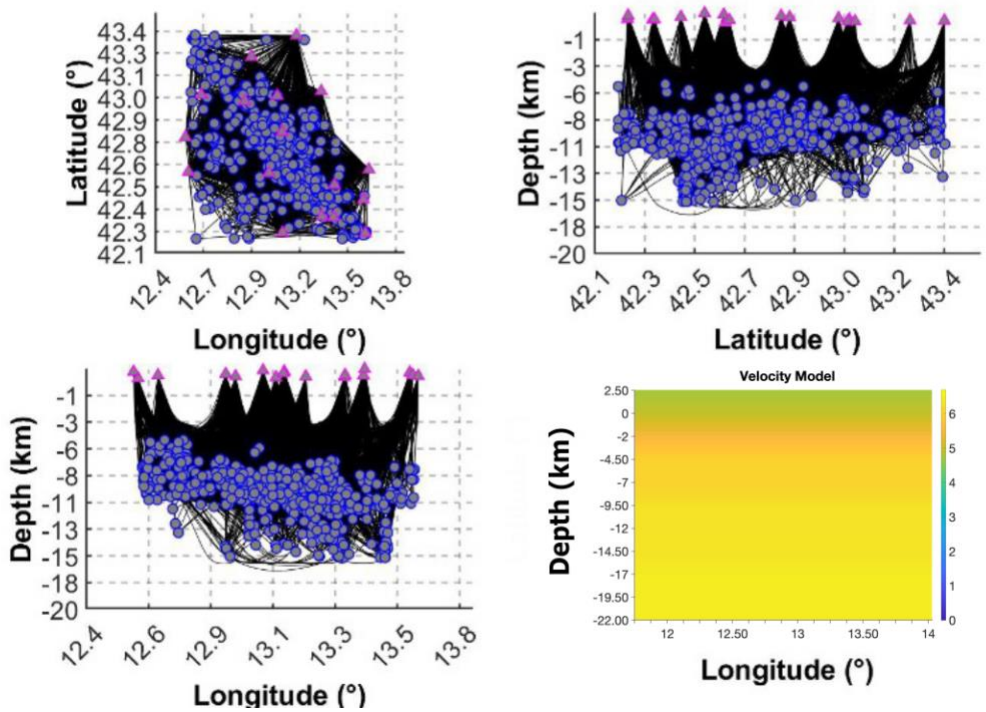

Figure S1. Ray coverage for the pre-sequence dataset and, on the right bottom corner, a vertical slice of the velocity model used for the analysis

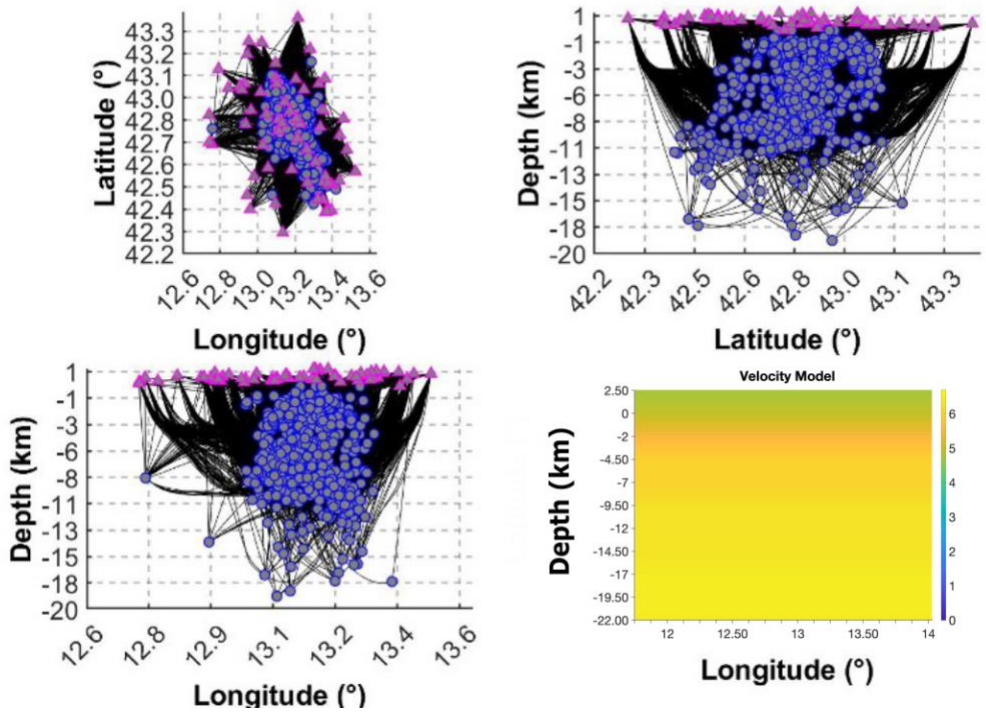

Figure S2. Ray coverage for the 2016-2017 sequence dataset and, on the right bottom corner, a vertical slice of the velocity model used for the analysis

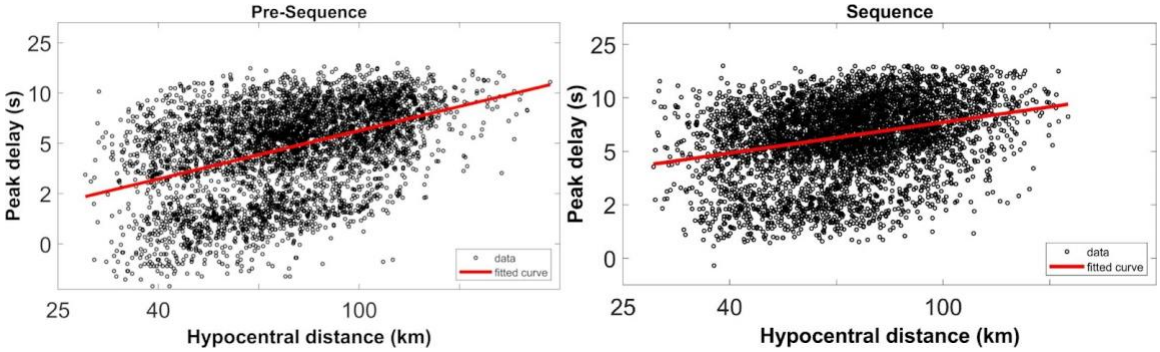

Figure S3. Log–log plot of peak delay (s) as a function of the hypocentral distances (km) for the pre-sequence and the 2016–2017 sequence at 1.5 Hz. The red solid line represents the best linear fit for the peak delay measurement (black circles).

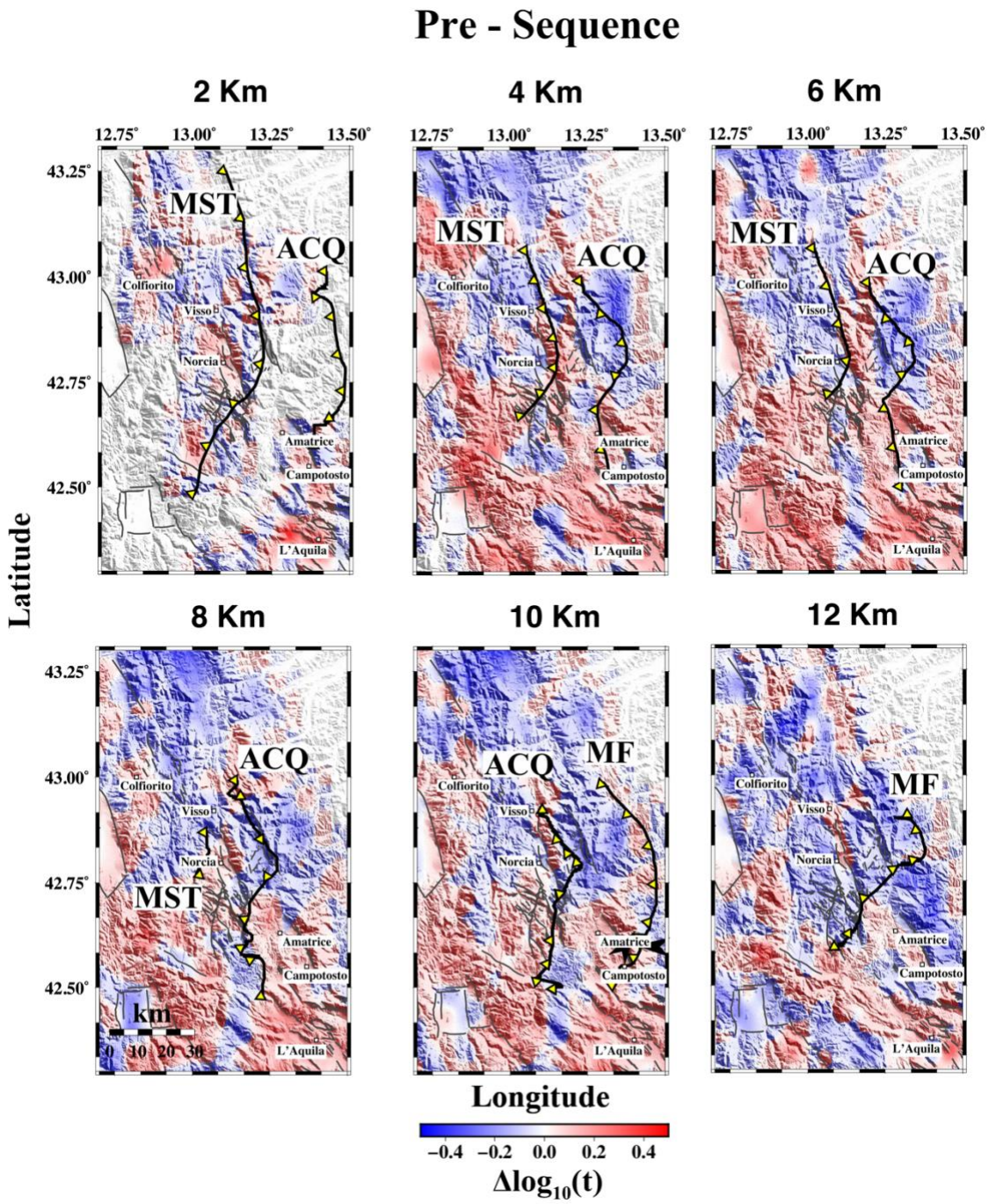

Figure S4. Spatial variation of the peak delay for the pre-sequence every 2 km depth, at a frequency band = 1.5 Hz. Gray lines are the faults from the ITHACA catalog; the black lines with yellow triangles are the thrusts of the Monti Sibillini (MST), Acquasanta (ACQ) and Montagna dei Fiori (MF).

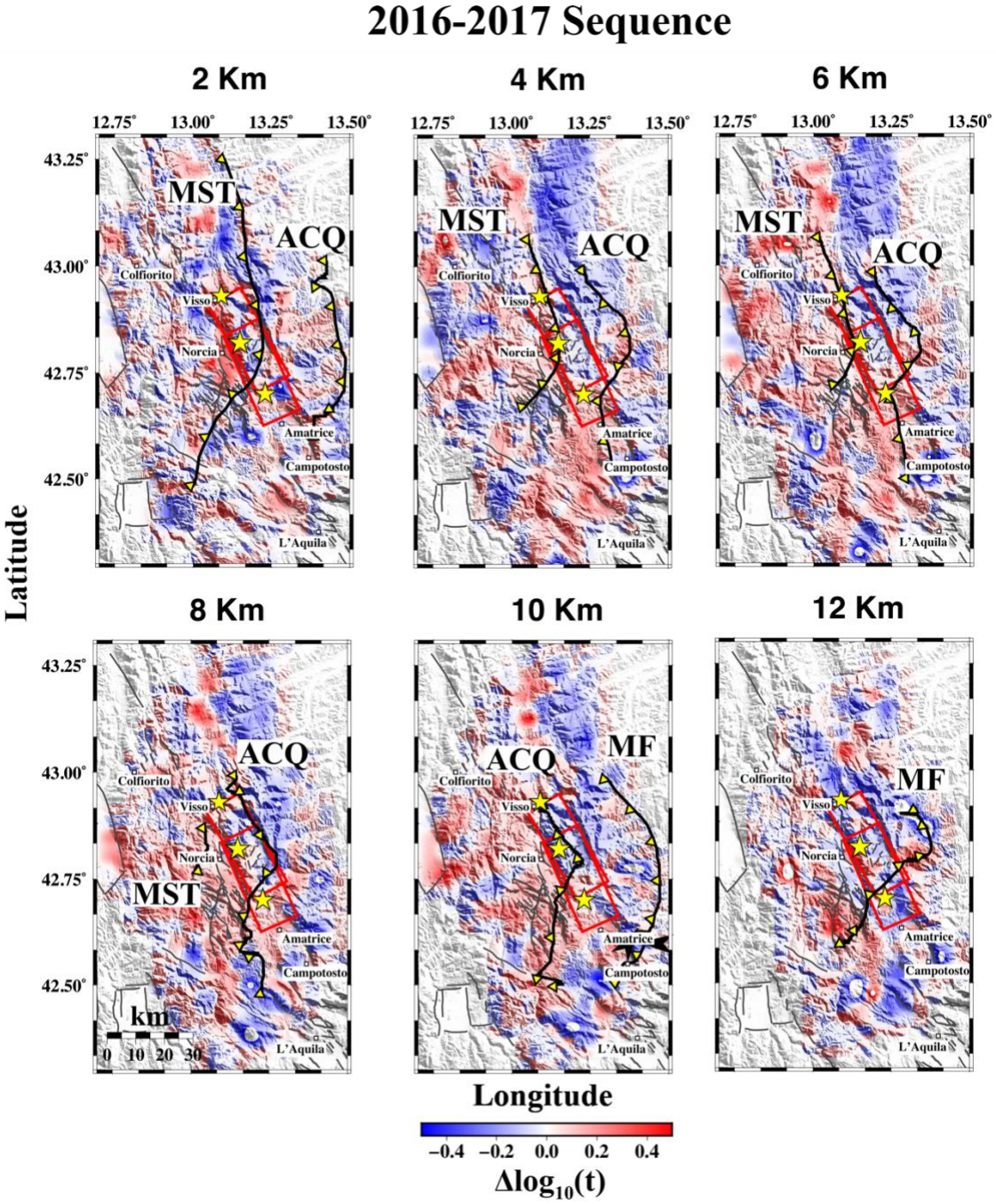

Figure S5. Spatial variation of the peak delay for the 2016-2017 sequence every 2 km depth, at a frequency band = 1.5 Hz. Yellow stars are the mainshock of the Amatrice-Visso-Norcia 2016-2017 seismic sequence; the red boxes represent the fault polygons for the 24 August Amatrice M6.0 and 30 October Norcia M6.5 earthquakes; gray lines are the faults from the ITHACA catalog; the black lines with yellow triangles are the thrusts of the Monti Sibillini (MST), Acquasanta (ACQ) and Montagna dei Fiori (MF).

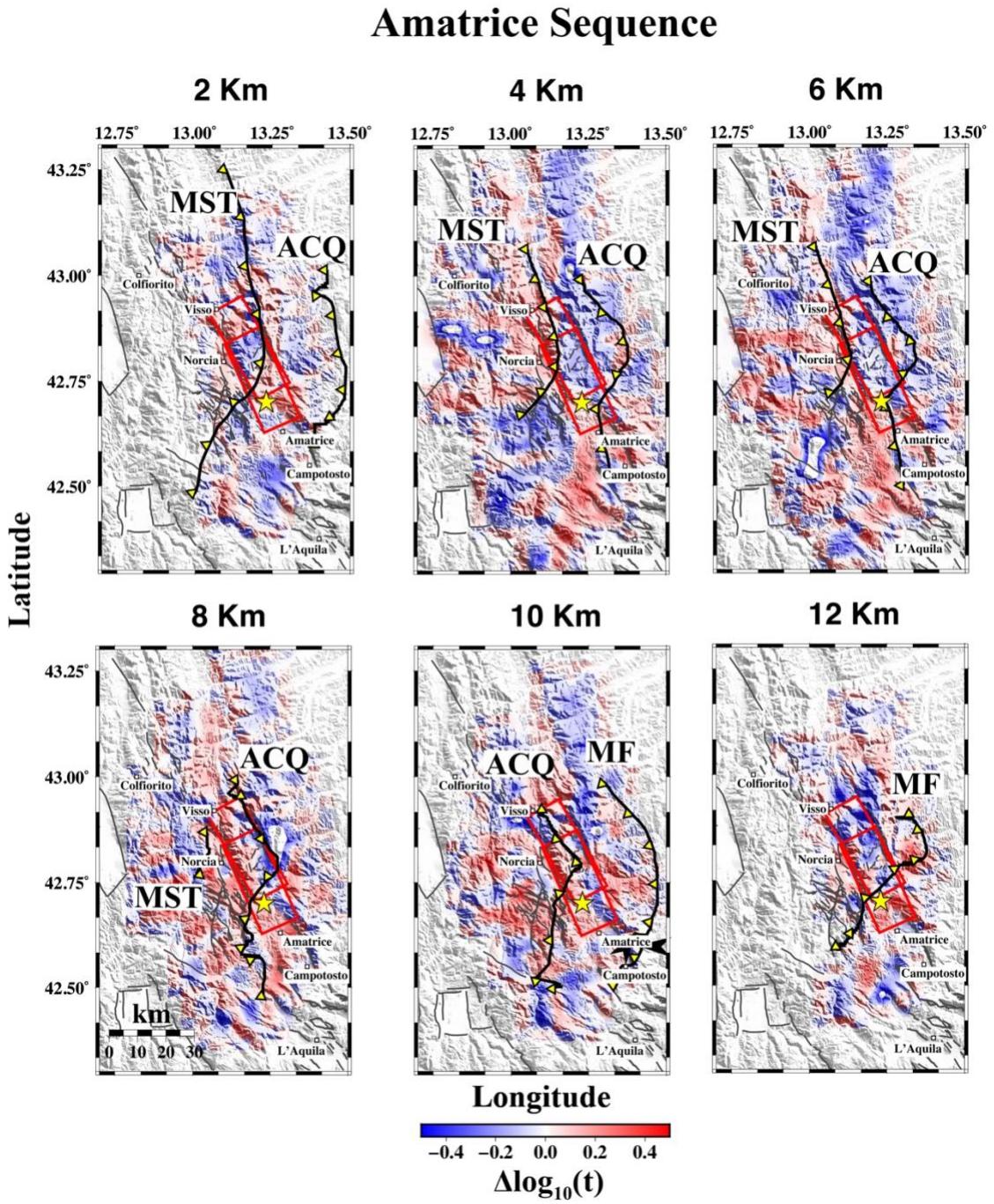

Figure S6. Spatial variation of the peak delay for the Amatrice sequence every 2 km depth, at a frequency band = 1.5 Hz. Yellow star is the mainshock of the Amatrice seismic sequence; the red boxes represent the fault polygons for the 24 August Amatrice M6.0 and 30 October Norcia M6.5 earthquakes; gray lines are the faults from the ITHACA catalog; the black lines with yellow triangles are the thrusts of the Monti Sibillini (MST), Acquasanta (ACQ) and Montagna dei Fiori (MF).

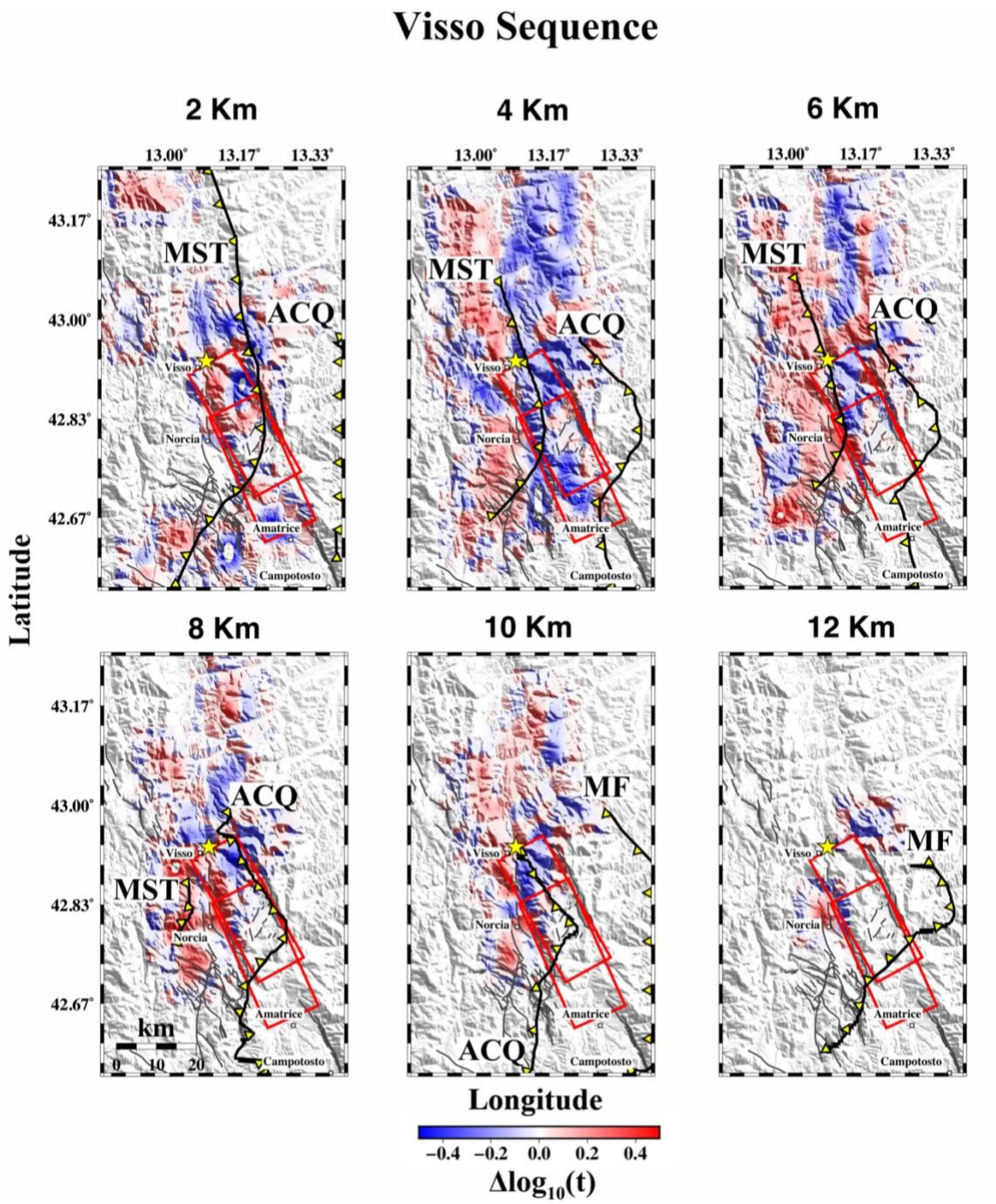

Figure S7. Spatial variation of the peak delay for the Visso sequence every 2 km depth, at a frequency band = 1.5 Hz. Yellow stars are the mainshock of the Amatrice and Visso seismic sequences; the red boxes represent the fault polygons for the 24 August Amatrice M6.0 and 30 October Norcia M6.5 earthquakes; gray lines are the faults from the ITHACA catalog; the black lines with yellow triangles are the thrusts of the Monti Sibillini (MST), Acquasanta (ACQ) and Montagna dei Fiori (MF).

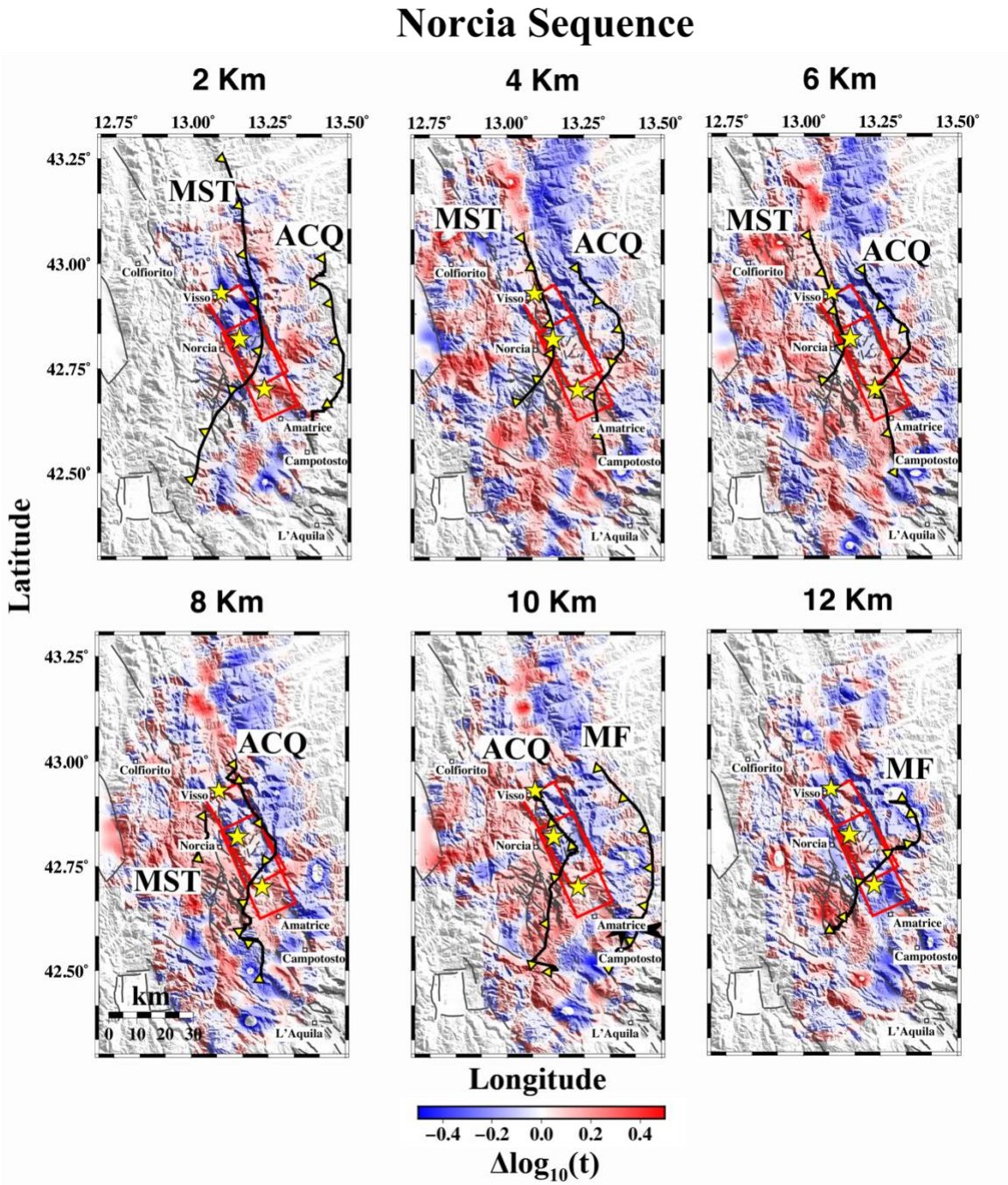

Figure S8. Spatial variation of the peak delay for the Norcia sequence every 2 km depth, at a frequency band = 1.5 Hz. Yellow stars are the mainshock of the Amatrice-Visso-Norcia seismic sequences; the red boxes represent the fault polygons for the 24 August Amatrice M6.0 and 30 October Norcia M6.5 earthquakes; gray lines are the faults from the ITHACA catalog; the black lines with yellow triangles are the thrusts of the Monti Sibillini (MST), Acquasanta (ACQ) and Montagna dei Fiori (MF).

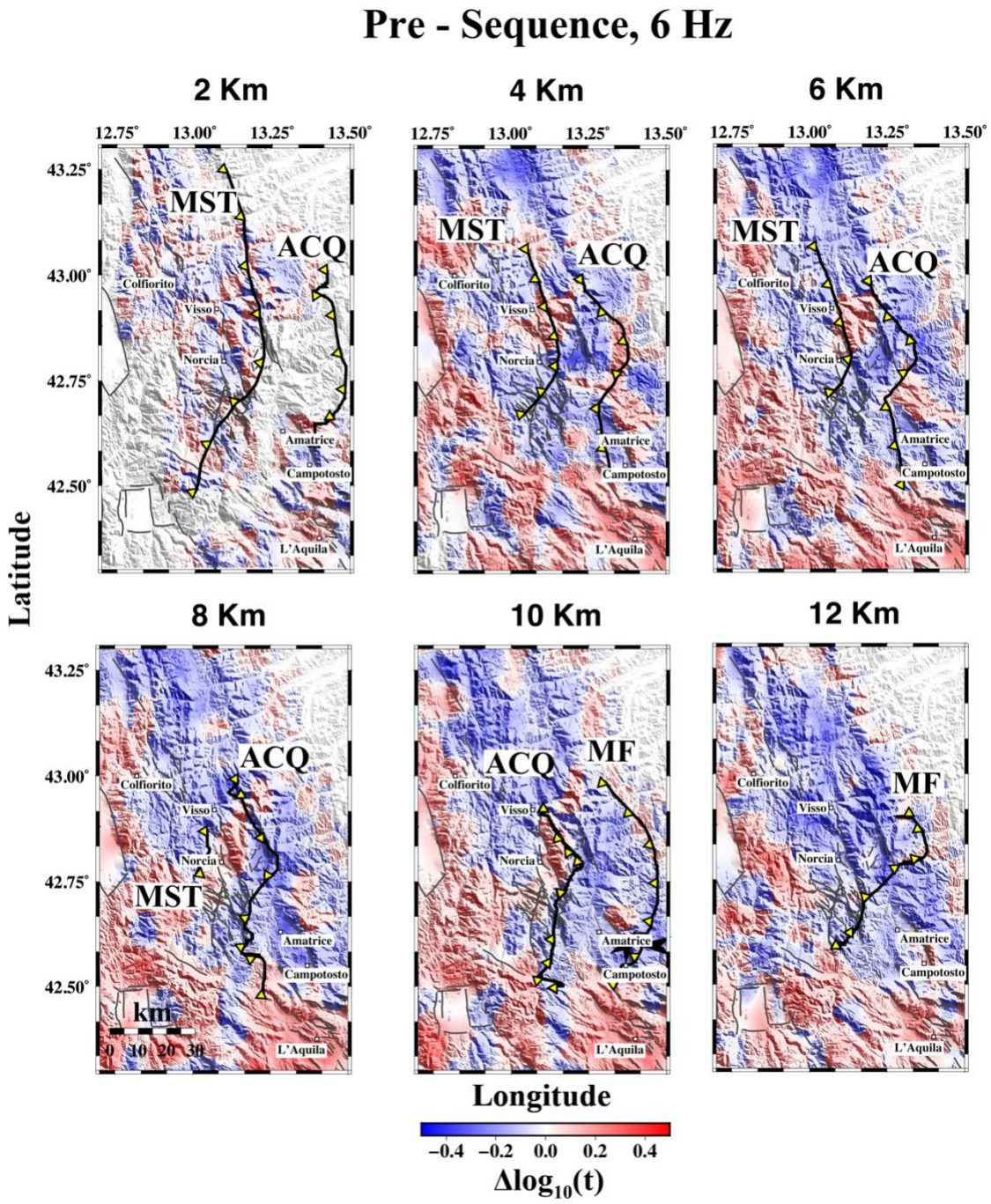

Figure S9. Spatial variation of the peak delay for the pre-sequence every 2 km depth, at a frequency band = 6 Hz. Gray lines are the faults from the ITHACA catalog; the black lines with yellow triangles are the thrusts of the Monti Sibillini (MST), Acquasanta (ACQ) and Montagna dei Fiori (MF).

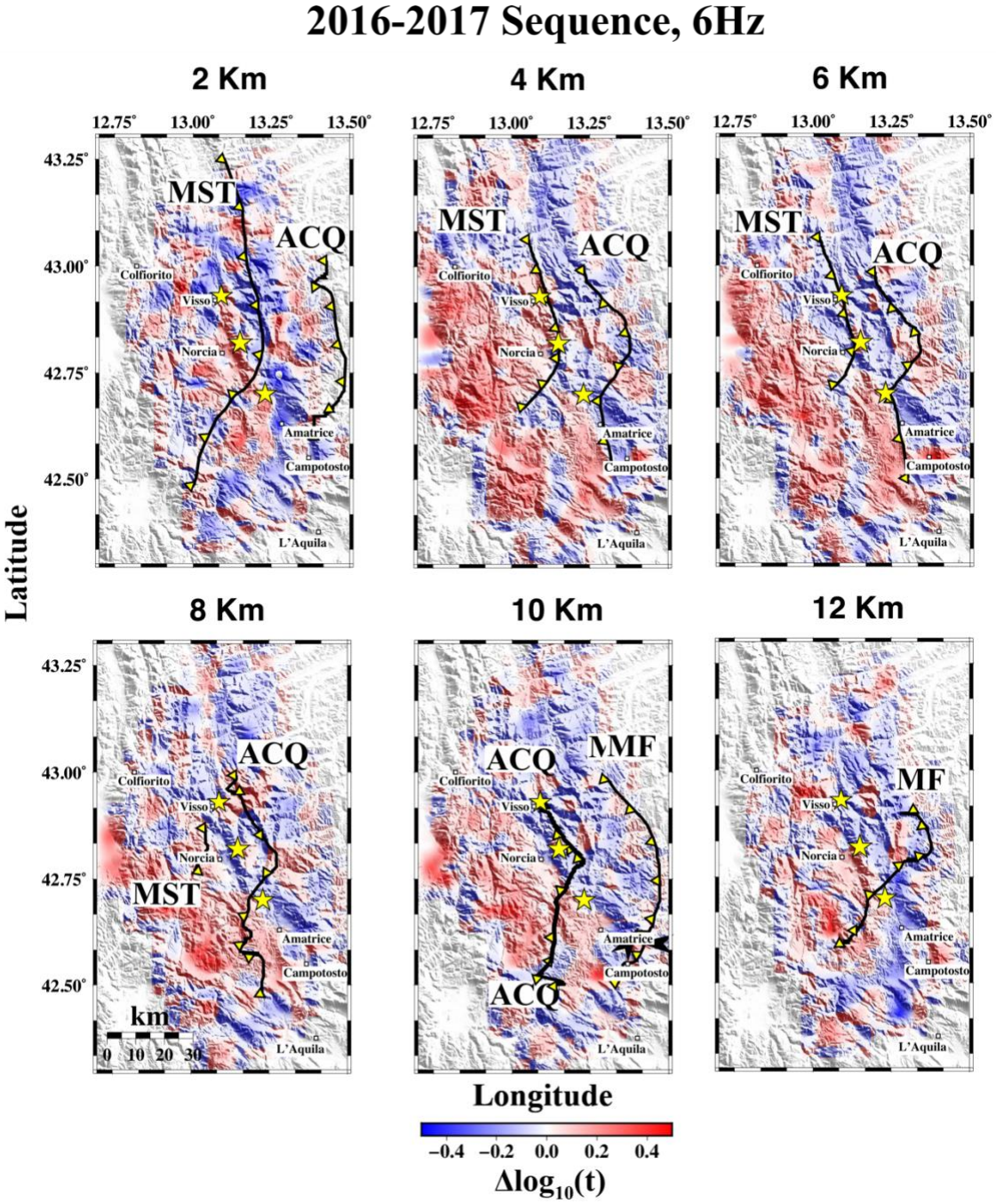

Figure S10. Spatial variation of the peak delay for the 2016-2017 sequence every 2 km depth, at a frequency band = 6 Hz. Yellow stars are the mainshock of the Amatrice-Visso-Norcia 2016-2017 seismic sequence; the red boxes represent the fault polygons for the 24 August Amatrice M6.0 and 30 October Norcia M6.5 earthquakes; gray lines are the faults from the ITHACA catalog; the black lines with yellow triangles are the thrusts of the Monti Sibillini (MST), Acquasanta (ACQ) and Montagna dei Fiori (MF).

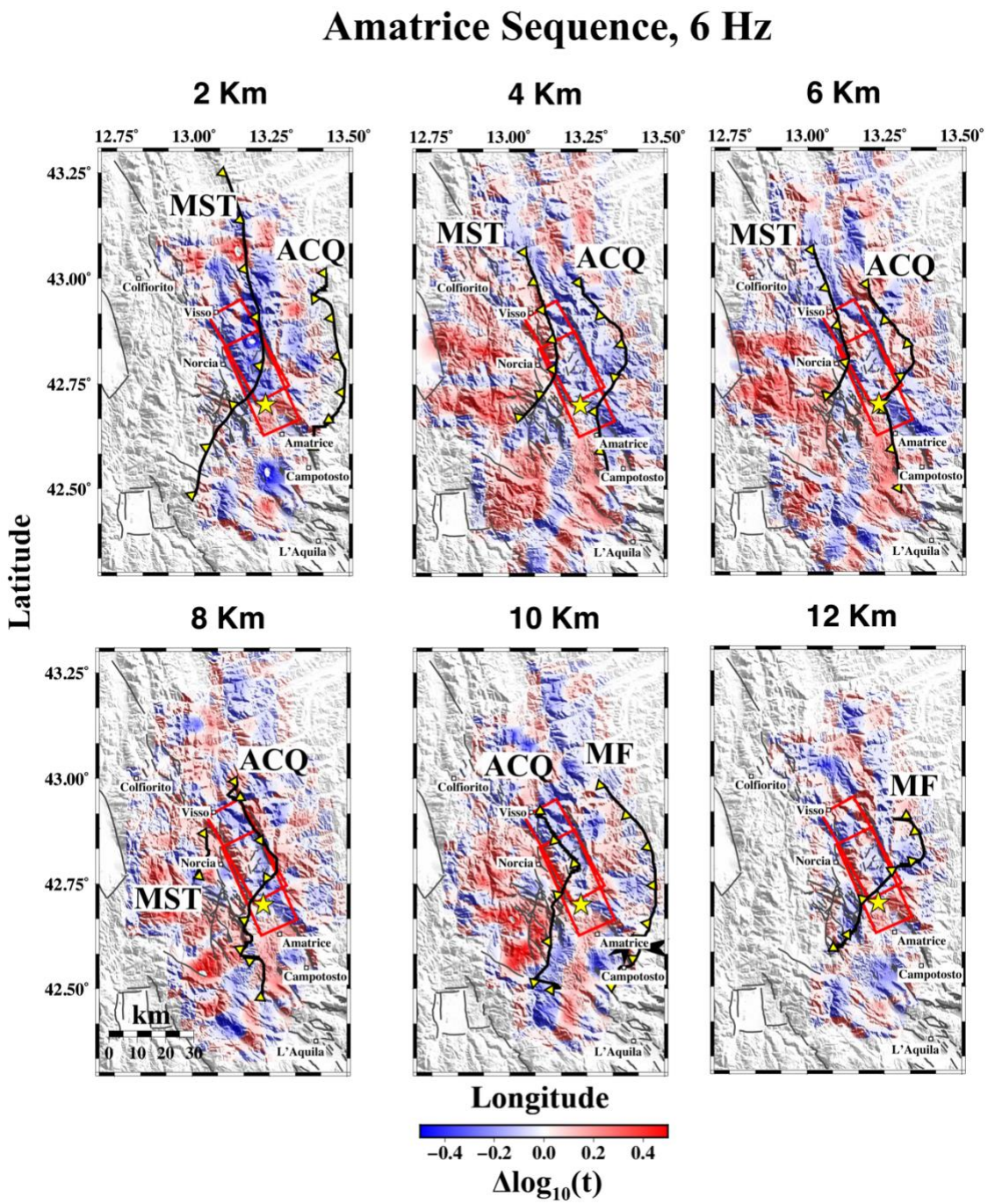

Figure S11. Spatial variation of the peak delay for the Amatrice sequence every 2 km depth, at a frequency band = 6 Hz. Yellow star is the mainshock of the Amatrice seismic sequence; the red boxes represent the fault polygons for the 24 August Amatrice M6.0 and 30 October Norcia M6.5 earthquakes; gray lines are the faults from the ITHACA catalog; the black lines with yellow triangles are the thrusts of the Monti Sibillini (MST), Acquasanta (ACQ) and Montagna dei Fiori (MF).

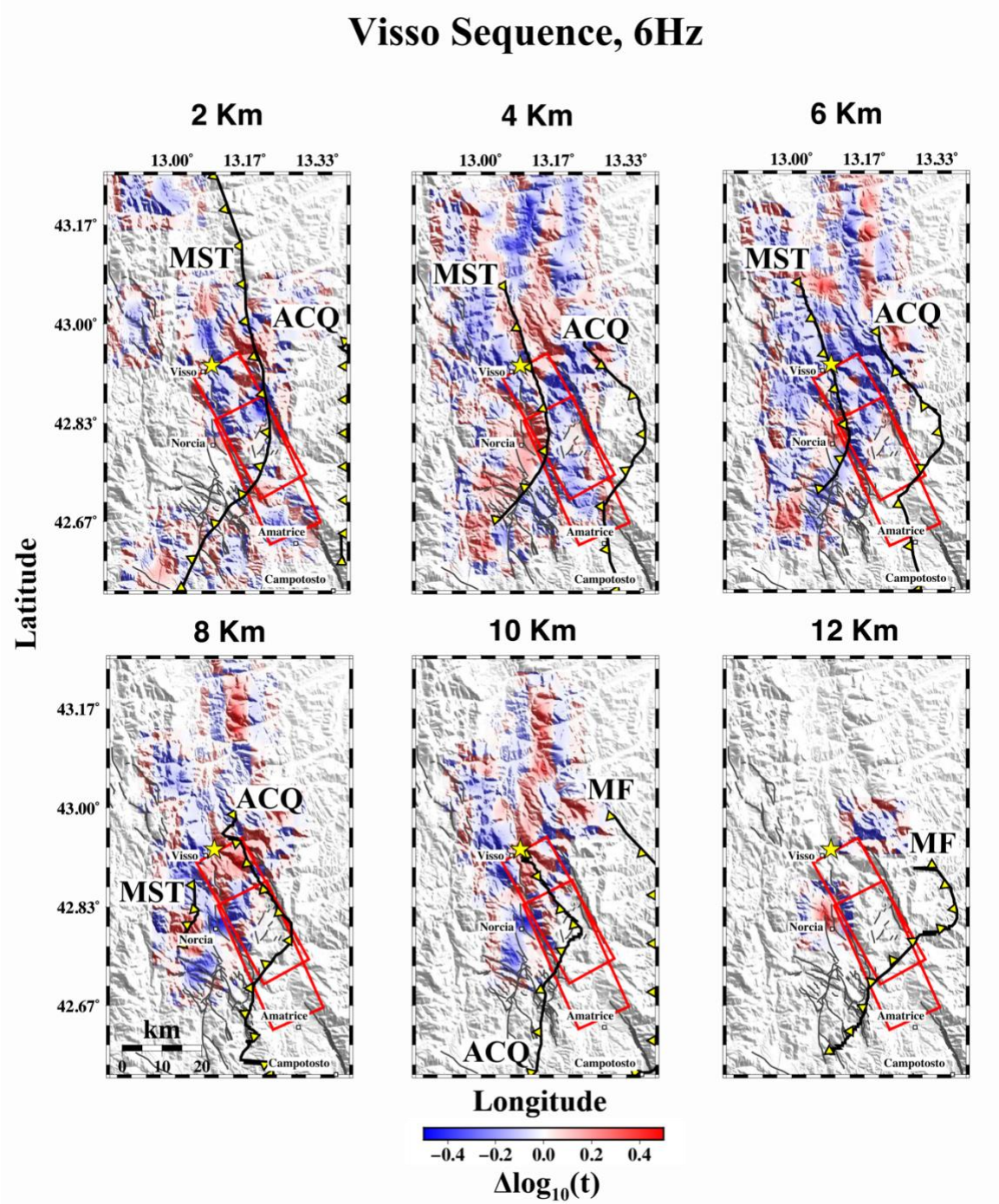

Figure S12. Spatial variation of the peak delay for the Visso sequence every 2 km depth, at a frequency band = 1.5 Hz. Yellow stars are the mainshock of the Amatrice and Visso seismic sequences; the red boxes represent the fault polygons for the 24 August Amatrice M6.0 and 30 October Norcia M6.5 earthquakes; gray lines are the faults from the ITHACA catalog; the black lines with yellow triangles are the thrusts of the Monti Sibillini (MST), Acquasanta (ACQ) and Montagna dei Fiori (MF).

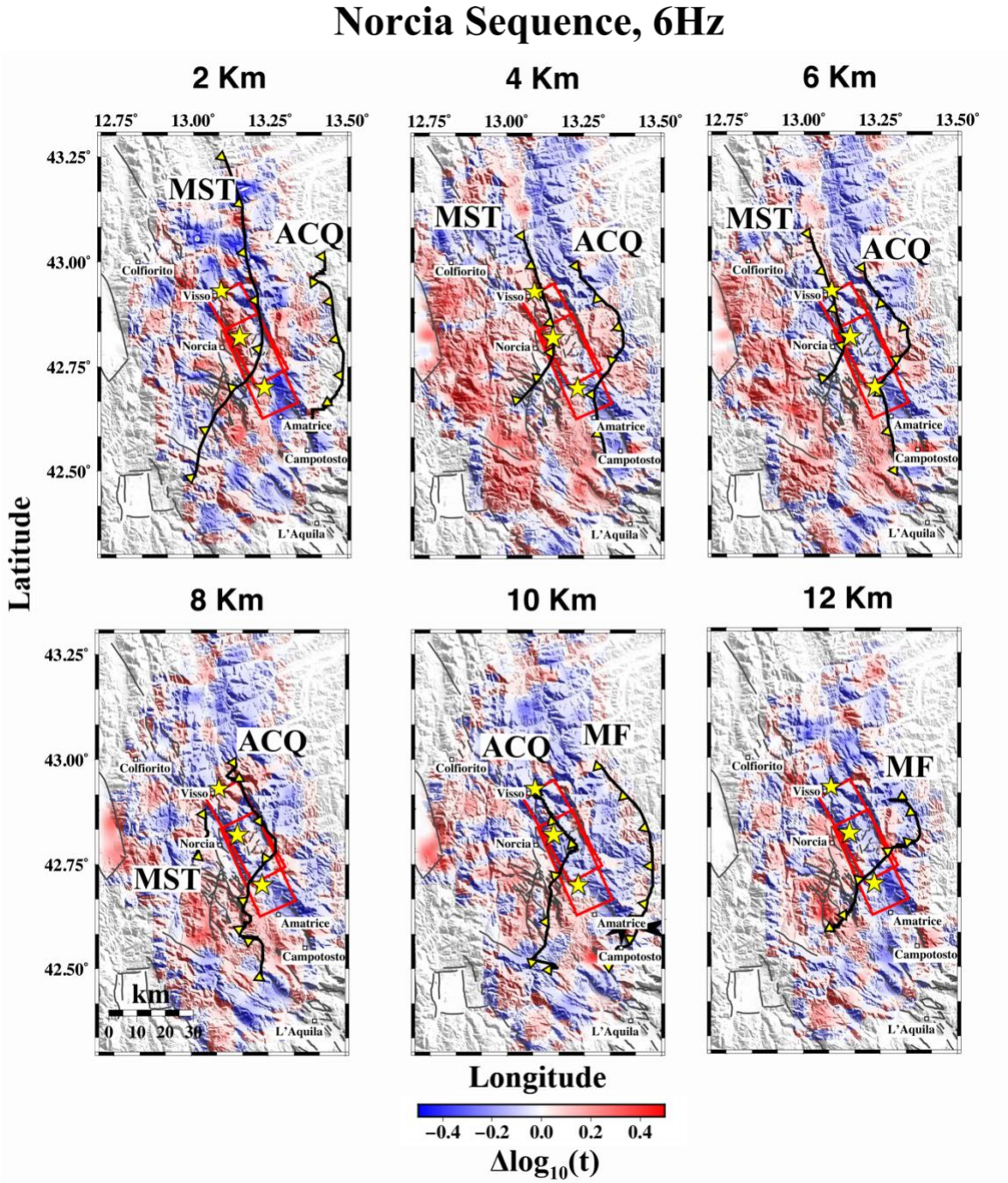

Figure S13. Spatial variation of the peak delay for the Norcia sequence every 2 km depth, at a frequency band = 6 Hz. Yellow stars are the mainshock of the Amatrice-Visso-Norcia seismic sequences; the red boxes represent the fault polygons for the 24 August Amatrice M6.0 and 30 October Norcia M6.5 earthquakes; gray lines are the faults from the ITHACA catalog; the black lines with yellow triangles are the thrusts of the Monti Sibillini (MST), Acquasanta (ACQ) and Montagna dei Fiori (MF).